GBT MEMO 98

National Radio Astronomy Observatory
Charlottesville, Virginia

PROFILE CORRUGATED HORN FOR THE GBT: PROTOTYPE DESIGN AND MEASUREMENT

S. Srikanth

January 25, 1993

Table 1 from GBT Memo No. 66 [1] gives the frequency breakups of the proposed Gregorian focus receivers for the GBT. This plan calls for wideband feeds and polarizers of bandwidth ratio of about 1.5 to 1, at the lowest five bands (1.15-1.73, 1.73-2.60, 2.60-3.95, 3.95-5.85 and 5.85-8.20 GHz). At the lowest three bands, the physical dimensions and weight of conventional conical corrugated horns become prohibitive. Hence, specially profiled, compact, corrugated horns will be used at these bands. The profile horn design has been used at L-band on the VLBA. However, this horn is a narrow band design (1.35:1 bandwidth ratio). The linear taper of the interior corrugated surface in a conical horn is replaced with a continuously curved profile in the case of the profile horn. The GBT requires a feed illumination taper of -15 dB at the edge of the subreflector for the Gregorian feeds up to 8.2 GHz and a -13 dB taper for feeds above 8.2 GHz [2]. For a -15 dB taper, a profile horn would have an aperture diameter of 56% and length of 85% of a linear taper horn. However, the penalty in the profile horn is the continuous conversion of the HE_{11} mode to higher order modes along the changing profile. Of importance are the highly cross-polarized EH_{12} mode which is dominant at the upper part of the band, and the HE_{12} mode which distorts the copolar pattern. For these reasons, we have used the profile horn design only where it is absolutely necessary.

Design:

The profile horn has three sections: namely, the input taper, the mode converter and the profile section. The input taper is a circular waveguide transition between the input waveguide radius and the mode converter radius. The mode converter transforms the fundamental TE_{11} mode in the circular waveguide to the HE_{11} mode in the corrugated waveguide. The profile section connecting the mode converter output to the aperture of the horn provides a frequency transition from the mode converter design frequency (f_i) to the HE_{11} mode balance frequency (f_o). In the mode converter, when conventional constant-width slots are used, the depth of the slots decreases from about one-half wavelength at f_i at the input to one-quarter wavelength at its output. These deep slots lead to the excitation of higher order modes which limits the high frequency performance. Ring-loaded slots [3] have been shown to be capacitive over a wider bandwidth than that which can be achieved by conventional constant-width slots. Hence, for the GBT wideband horns, ring-loaded slots have been used in the mode converter. The profile section has constant-width slots which vary in depth from one-quarter of wavelength at f_i at the input to one-quarter of wavelength at f_o at the aperture of the horn.

Figure 1 gives the dimensions of the profile horn at L-band (1.15-1.73 GHz). The length of the horn from the first slot in the converter to the aperture is 106.8". Two different lengths have been used for the input taper, as discussed in the next section. With the longer taper, the total length of the horn is 140". The aperture of the horn has an inside diameter of 49.5". The mode converter has eight ring-loaded slots and has an inside slope of 6°. The slot density throughout the length of the horn is eight per wavelength at f_1. The profile section of the horn varies in slope from 6° at the converter end through a maximum of 15° to 0° at the aperture.

Measurement on the Prototype Feed:

A prototype feed of the profile horn was machined in the Green Bank machine shop. The prototype was built at C-band (4.3-6.5 GHz), as a compromise between size and ease of measuring at the Green Bank Antenna Range. The field patterns of the horn were measured in the principal planes. All the results are referred to in equivalent frequencies at L-band rather than the actual frequencies of measurement. The actual frequency is shown in parentheses. Figures 2, 3 and 4 show the patterns at the equivalent frequencies of 1.15 GHz (4.311 GHz), 1.40 GHz (5.248 GHz) and 1.73 GHz (6.486 GHz). The illumination taper at 15° (edge of the subreflector) varies between -13.5 to -15.0 dB below the peak. There is excellent match of the pattern in the two planes. Cross-polarization was measured in the 45° plane and is shown in Figure 5. The worst cross-polarization occurs at 1.60 GHz (5.998 GHz) where it is -28.5 dB below the peak of the main beam, as shown in Table 2. Using the measured patterns, the aperture efficiency and the spillover temperature at 90° elevation of the telescope are calculated. The Gain/T_{system} value is given by

$$\text{Gain}/T_{sys} = \frac{A_p * \eta}{2760 * T_{sys}} \quad (\text{Jy}^{-1})$$

where A_p is the projected aperture in m^2, η is the aperture efficiency and T_{system} is the sum of receiver, sky and spillover temperatures. A value of 7 K is assumed for the receiver temperature and 6 K for the sky temperature. Table 2 lists aperture efficiency, T_{system} and Gain/T_{system} at different frequencies.

The location of the phase center of the feed with frequency was also measured. At 1.15 GHz, the phase center is 3.6λ inside from the aperture, at 1.40 GHz 7.4λ and at 1.73 GHz, it is 10.2λ.

A waveguide section with zero slope and having two corrugations was machined to be attached at the aperture end of the feed. The purpose of this was to limit the travel of the phase center of the feed with frequency. The illumination taper at 15° varied between -14.1 and -15.6 dB from 1.15 GHz to 1.73 GHz. The phase center travelled by about the same amount as the case without this extension piece. Hence, there seems to be no advantage to having this additional section of waveguide at the aperture of the feed.

The input return loss was measured with four different input tapers. The length of the first taper is 10 times its smaller radius as per [4] and will be 33.140" long at L-band. The slope of the taper is 0° at the input and 6° at the converter end to match the slope of the converter. The second, third and fourth tapers are 2 wavelengths long at the lowest frequency and will be 20.550" long at L-band. The second taper has a hyperbolic secant profile with zero slope at the input and a slope of 6° at the output. The third and fourth tapers have zero slopes on either end. The third is a sine squared curve while the fourth is a curve based on [5]. The results of the measurements are given in Figures 6 and 7. The longer taper (Figure 6a) gives the best performance with return loss exceeding 35 dB in the 1.15 GHz to 1.73 GHz range. At 1.10 GHz (4.124 GHz), the return loss is 28.3 dB. All the shorter tapers have return loss no less than 30 dB in the required frequency range. The deterioration is mainly at the low end of the band. At 1.10 GHz, tapers #2, #3 and #4 have return loss of 19.4, 18.7 and 23.8 dB, respectively. Taper #2 is about 5 dB better than taper #4 within the frequency range of interest. All the results in Table 2 are measurements made with the long taper. However, the shorter taper does have an effect on the cross-polarization levels. Measurements done with taper #2 indicate about 1 dB deterioration of cross-polarization levels as compared to that shown in Table 2.

Measurements of copolar far-field patterns were done at 1 GHz (3.749 GHz) and up to 2.00 GHz (7.498 GHz). The illumination tapers at 15° at these frequencies are shown in Table 2. Cross-polar field was also measured and was found to be at least -28.5 dB below the copolar peak at all frequencies, except at 2.00 GHz where it is -25 dB.

Thin Vane Design:

The ratio of the thickness of the vane between slots to the slot pitch for the prototype feed is 0.25, making the thickness of the vanes at L-band equal to 0.322". If this design is used for the L-band feed, F. Crews and M. Barkley suggest using aluminum honeycomb with sheet metal on either side for the fabrication of the vanes. The other alternative is to use sheet metal for the vanes, in which case the vane thickness should be small. R. Norrod has estimated that the weight of an L-band feed with thin sheet metal vanes of thickness 0.080" would be the same as the feed with honeycomb vanes. A prototype with thin vanes was built at C-band. The thickness of the vanes in this prototype would scale to 0.090" in the L-band feed.

Detailed measurements done on this feed indicate no change in copolar patterns within measurement errors. The cross-polar levels are about the same as the first prototype up to 1.73 GHz. From 1.73 GHz to 2.00 GHz, there is deterioration of cross polarization by about 1.3 dB. Return loss of this feed was measured with input taper #2 and is shown in Figure 8. Return loss, in this case, is not as good as in Figure 6(b), specifically at the higher end of the band; however, it is no lower than 30 dB from 1.15 GHz to 1.86 GHz.

Conclusion:

The prototype feed has excellent return loss in the desired frequency range. The saving in length by using a shorter taper is almost 13" with return loss still quite good. The shorter tapers #2 and #4 will be measured with the prototype orthomode transducer, and one of the two tapers can be chosen after this measurement.

The field patterns have excellent symmetry in the two principal planes. The feed could be used with very little additional loss down to 1.10 GHz.

The second prototype feed with thin vanes has very similar performance as the first prototype feed in the 1.10 to 1.75 GHz frequency range. Since NRAO has previous experience with the fabrication process of the thin vane design (VLBA L-band feed), this design will be used in the L-band feed.

I would like to acknowledge the contributions of M. Barkley, G. Behrens, F. Crews, R. Hanshew, R. Norrod, F. Schwab and W. Sizemore to the design, fabrication and measurement of this feed.

References:

[1] M. Balister, R. Norrod and S. Srikanth, "Gregorian Receivers for the GBT," GBT Memo No. 66, Sept. 10, 1991.

[2] S. Srikanth, "Gain/System Temperature Optimization at Secondary Focus," GBT Memo No. 87, Oct. 6, 1992.

[3] Y. Takeichi, T. Hashimoto and F. Takeda, "The Ring-Loaded Corrugated Waveguide," *IEEE Trans. Microwave Theory Tech.*, vol. MTT-19, pp. 947-950, Dec. 1971.

[4] B. MacA. Thomas, G. L. James and K. J. Greene, "Design of Wideband Corrugated Conical Horns for Cassegrain Antennas," *IEEE Trans. Antennas Propagat.*, vol. AP-34, pp. 750-757, 1986.

[5] H. J. Gould, A. E. Smoll and C. C. Han, "New Non-Uniform Waveguide Taper Design Yielding Low VSWR and High Rejection," in *Proc. IEEE MTT-S Int. Microwave Symp.*, pp. 221-223, 1973.

TABLE 1

GBT RECEIVER PLAN

RX NR.	BAND	FEED GHz LOW	FEED GHz HIGH	TYPE	BW RATIO	WG DIA Inches	Flo/Fco	Fco GHz	Fhom GHz	RECEIVER GHz LOW	RECEIVER GHz HIGH	BW RATIO	POLARIZATION
1	L	1.15	1.73	Profile	1.50	6.628	1.10	1.04	1.73	1.15	1.73	1.50	Dual Linear
2		1.73	2.60	Profile	1.50	4.406	1.10	1.57	2.60	1.73	2.60	1.50	Dual Linear
3	S	2.60	3.95	Profile	1.52	2.932	1.10	2.36	3.91	2.60	3.95	1.52	Dual Linear
4		3.95	5.85	Lin.Taper	1.48	1.930	1.10	3.58	5.95	3.95	5.85	1.48	Dual Linear
5	C	5.85	8.20	Lin.Taper	1.40	1.303	1.10	5.31	8.81	5.85	8.20	1.40	Dual Linear
6	X	8.00	10.00	Lin.Taper	1.25	1.024	1.18	6.76	11.20	8.00	10.00	1.25	Dual Circular
7		10.00	12.40	Lin.Taper	1.24	0.769	1.11	9.00	14.92	10.00	12.40	1.24	Dual Circular
8	Ku	12.00	15.40	Lin.Taper	1.28	0.700	1.21	9.88	16.39	12.00	15.40	1.28	Dual Circular
9		15.40	18.00	Lin.Taper	1.17	0.499	1.11	13.86	22.98	15.40	18.00	1.17	Dual Circular
10	K	18.00	22.00	Lin.Taper	1.22	0.427	1.11	16.20	26.86	18.00	22.00	1.22	Dual Circular
11		22.00	26.50	Lin.Taper	1.20	0.349	1.11	19.79	32.83	22.00	26.50	1.20	Dual Circular
12	Ka	26.50	33.00	Lin.Taper	1.25	0.290	1.11	23.84	39.55	26.50	33.00	1.25	Dual Circular
13		33.00	40.00	Lin.Taper	1.21	0.233	1.11	29.69	49.25	33.00	40.00	1.21	Dual Circular
14	Q	40.00	45.50	Lin.Taper	1.14	0.192	1.11	35.99	59.70	40.00	45.50	1.14	Dual Circular
15		45.50	52.00	Lin.Taper	1.14	0.169	1.11	40.94	67.90	45.50	52.00	1.14	Dual Circular

TABLE 2

Equivalent Freq. (GHz)	Freq. of Measurement (GHz)	Illumination Taper at 15° (dB)		Cross-Polarization Below Peak (dB)	Calculated Efficiency %	T_{system} (K)	Calculated Gain/T_{system} (Jy^{-1})	Phase Center Distance From Aperture/ Wavelength
		E-Plane	H-Plane					
1.00	3.749	-9.97	-10.73	-29.2				
1.10	4.124	-12.70	-13.30	-30.5	67.31	18.9	0.1013	2.60
1.15	4.311	-13.37	-13.54	-33.0	70.92	18.4	0.1097	3.65
1.20	4.499	-14.31	-14.43	-36.0	66.88	17.0	0.1119	4.70
1.40	5.248	-14.93	-14.40	-40.0	65.87	17.2	0.1090	7.44
1.60	5.998	-13.98	-15.25	-28.5	60.47	16.3	0.1056	9.20
1.73	6.486	-14.66	-14.48	-30.0	64.74	16.7	0.1103	10.18
1.75	6.561	-15.25	-14.76	-30.5	65.19	15.8	0.1174	10.32
1.80	6.748	-16.63	-15.06	-30.0				
1.90	7.123	-19.07	-17.59	-28.5				
2.00	7.498	-17.92	-18.03	-25.0				

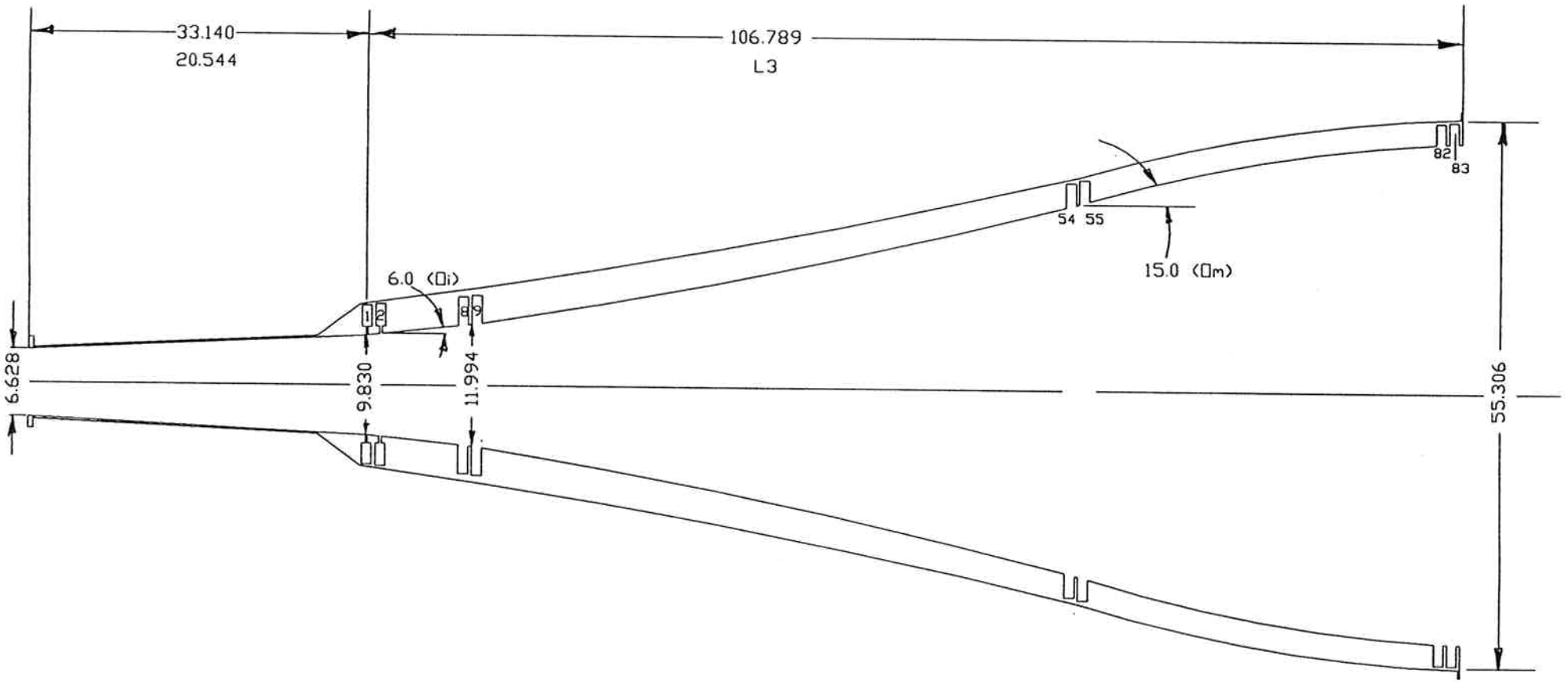

Fig. 1. GBT L-band profile horn.

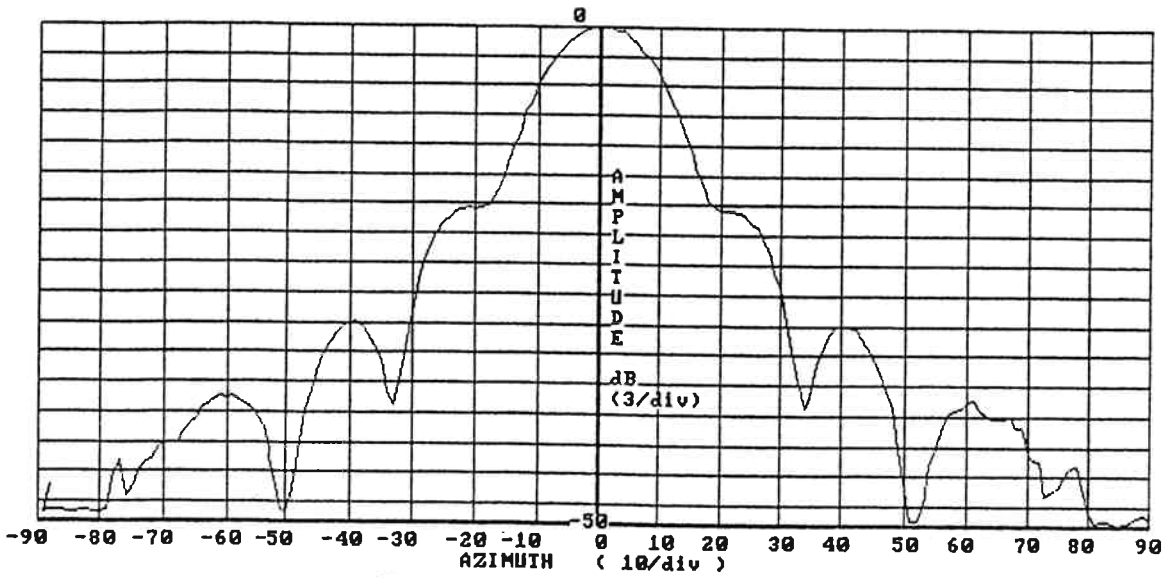

FOCUS = CASSEGRAIN EDGE ILLUMINATION : RIGHT = -2.54 LEFT = -2.87
FEED = L-Band Prototype (GBT) FREQ = 4.3110 (GHz) PLANE = E
COMMENTS : 1.15 GHz
DATE : 11/09/91

(a) E-plane

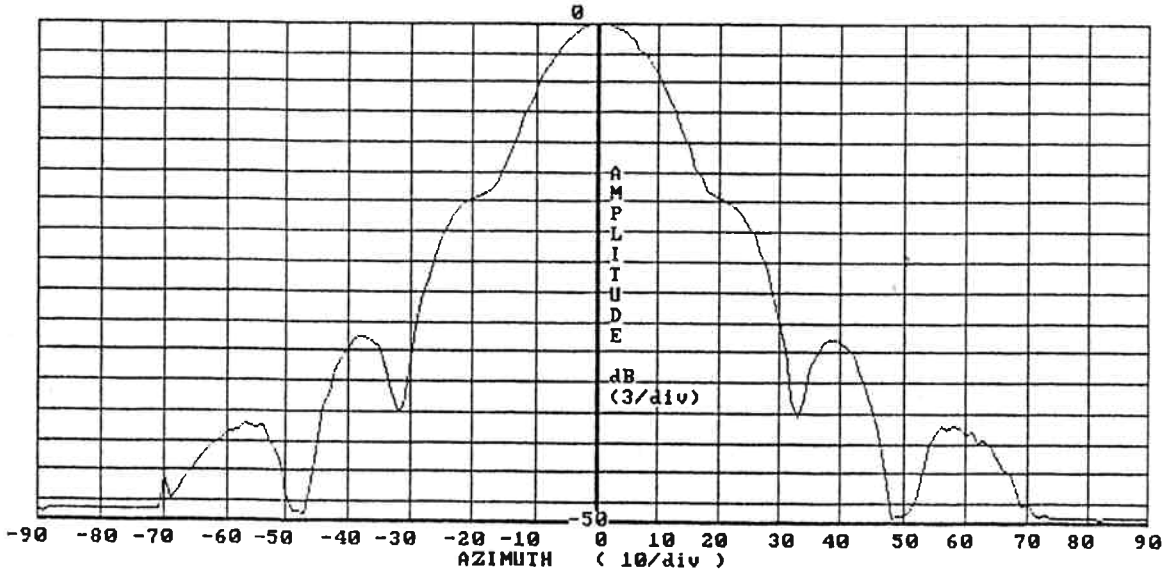

FOCUS = CASSEGRAIN EDGE ILLUMINATION : RIGHT = -2.65 LEFT = -3.23
FEED = L-Band Prototype (GBT) FREQ = 4.3110 (GHz) PLANE = H
COMMENTS : 1.15 GHz
DATE : 11/09/91

(b) H-plane

Fig. 2. Far-field pattern at 1.15 GHz (4.311 GHz).

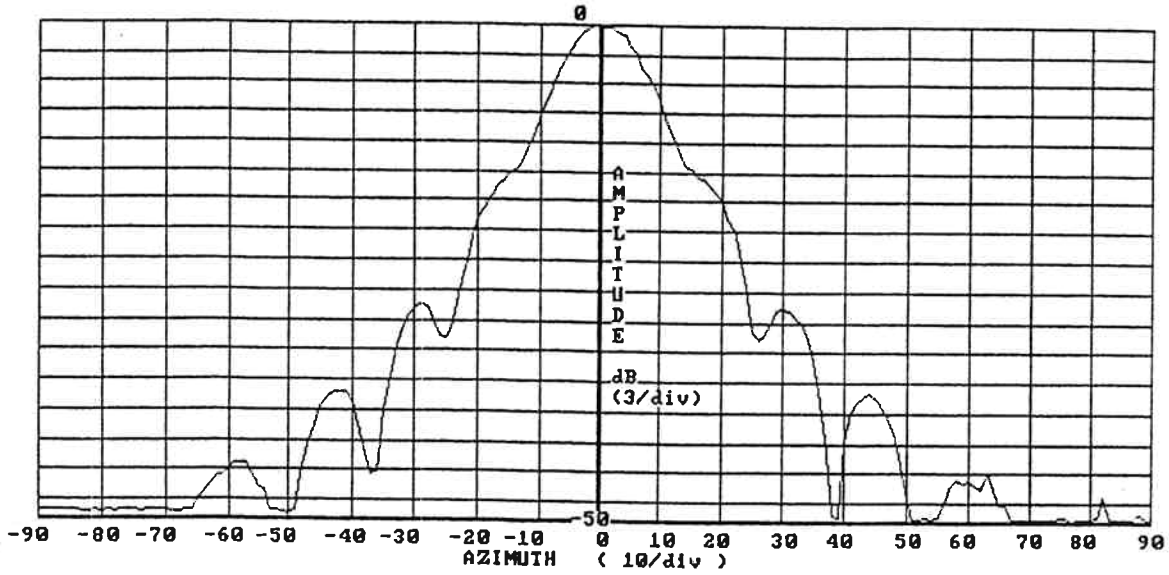

FOCUS = CASSEGRAIN EDGE ILLUMINATION : RIGHT = -4.34 LEFT = -4.49
FEED = L-Band Prototype (GBT) FREQ = 5.2480 (GHz) PLANE = E
COMMENTS : 1.40 GHz
DATE : 11/09/91

(a) E-plane

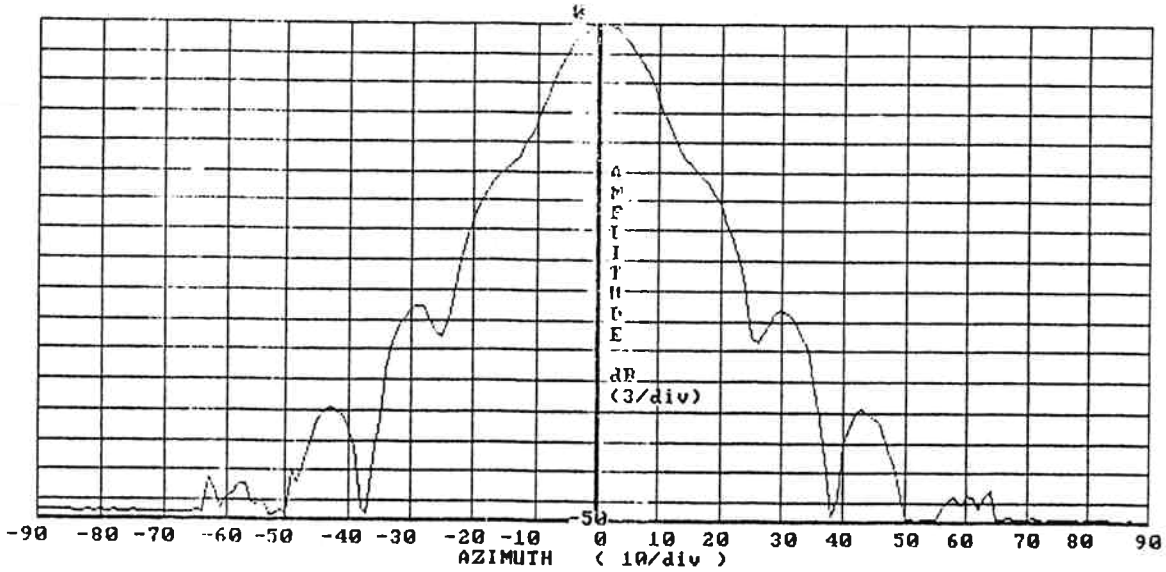

FOCUS = CASSEGRAIN EDGE ILLUMINATION : RIGHT = -3.68 LEFT = -4.81
FEED = L-Band Prototype (GBT) FREQ = 5.2490 (GHz) PLANE = H
COMMENTS : 1.40 GHz
DATE : 11/09/91

(b) H-plane

Fig. 3. Far-field pattern at 1.40 GHz (5.248 GHz).

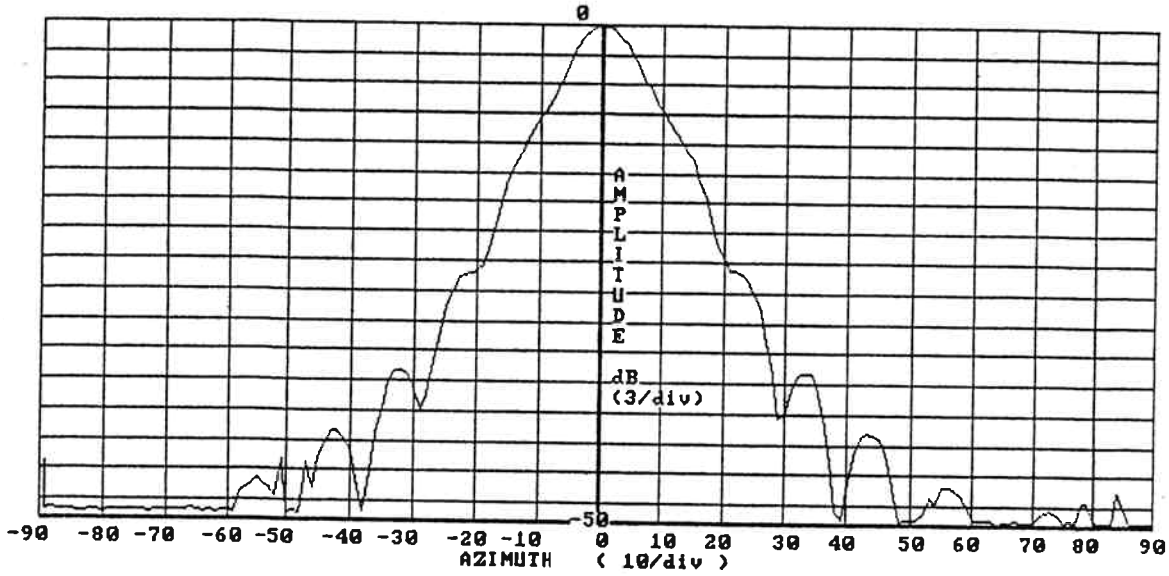

FOCUS = CASSEGRAIN EDGE ILLUMINATION : RIGHT = -5.54 LEFT = -6.07
FEED = L-Band Prototype (GBT) FREQ = 6.4860 (GHz) PLANE = E
COMMENTS : 1.73 GHz
DATE : 11/09/91

(a) E-plane

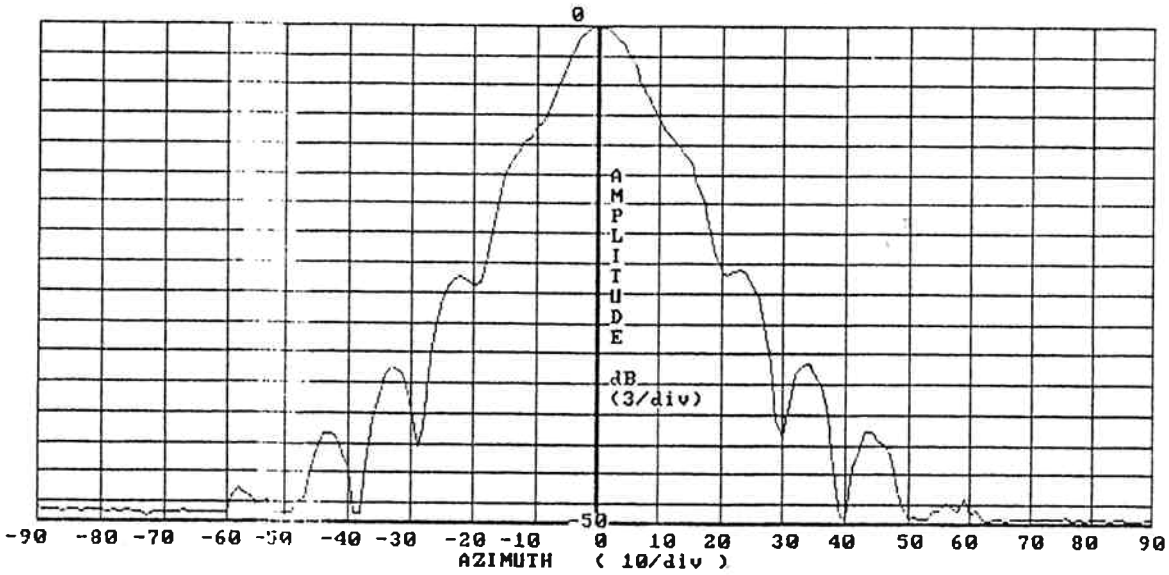

FOCUS = CASSEGRAIN EDGE ILLUMINATION : RIGHT = -5.97 LEFT = -6.64
FEED = L-Band Prototype (GBT) FREQ = 6.4860 (GHz) PLANE = H
COMMENTS : 1.73 GHz
DATE : 11/09/91

(b) H-plane

Fig. 4. Far-field pattern at 1.73 GHz (6.486 GHz).

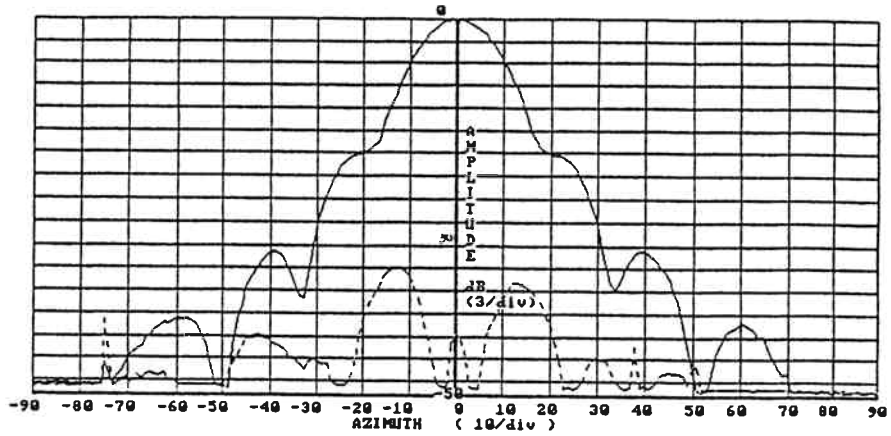

FOCUS = CASSEGRAIN EDGE ILLUMINATION : RIGHT = -41.00 LEFT = -40.21
FEED = L-Band Ptototype (CBT) FREQ = 4.311 (GHz) PLANE = 45
COMMENTS : 1.15
DATE : 12/07/91

(a)

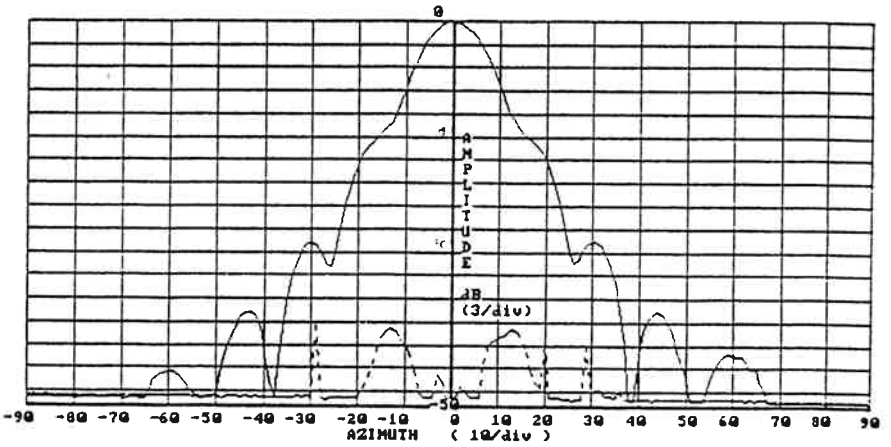

FOCUS = CASSEGRAIN EDGE ILLUMINATION : RIGHT = -44.36 LEFT = -48.17
FEED = L-Band Ptototype (CBT) FREQ = 5.2480 (GHz) PLANE = 45
COMMENTS : 1.400
DATE : 12/07/91

(b)

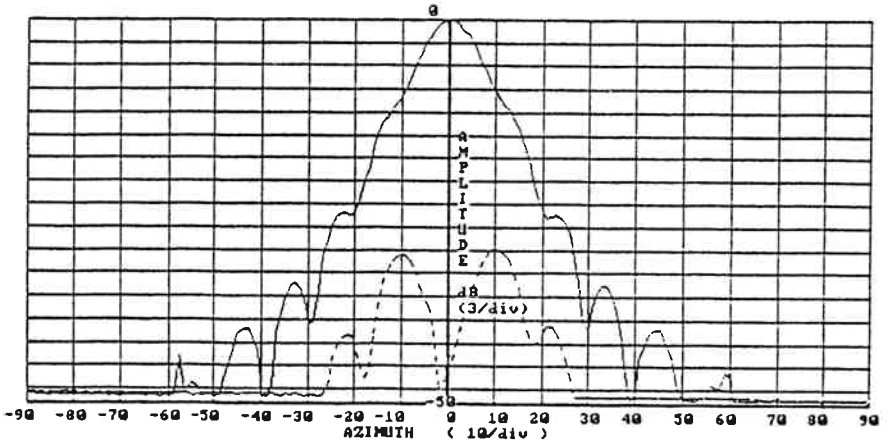

FOCUS = CASSEGRAIN EDGE ILLUMINATION : RIGHT = -32.15 LEFT = -32.83
FEED = L-Band Ptototype (CBT) FREQ = 6.4860 (GHz) PLANE = 45
COMMENTS : 1.73 GHz
DATE : 12/13/91

(c)

Fig. 5. Copolar and cross-polar field patterns in the 45° plane at (a) 1.15 GHz (4.311 GHz), (b) 1.40 GHz (5.248 GHz) and (c) 1.73 GHz (6.486 GHz).

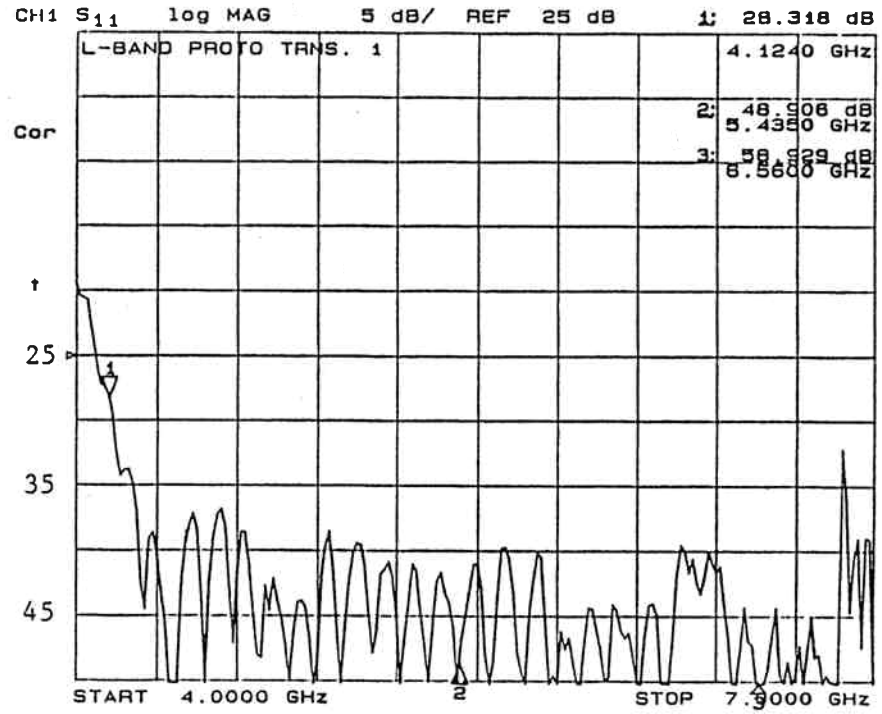

(a)

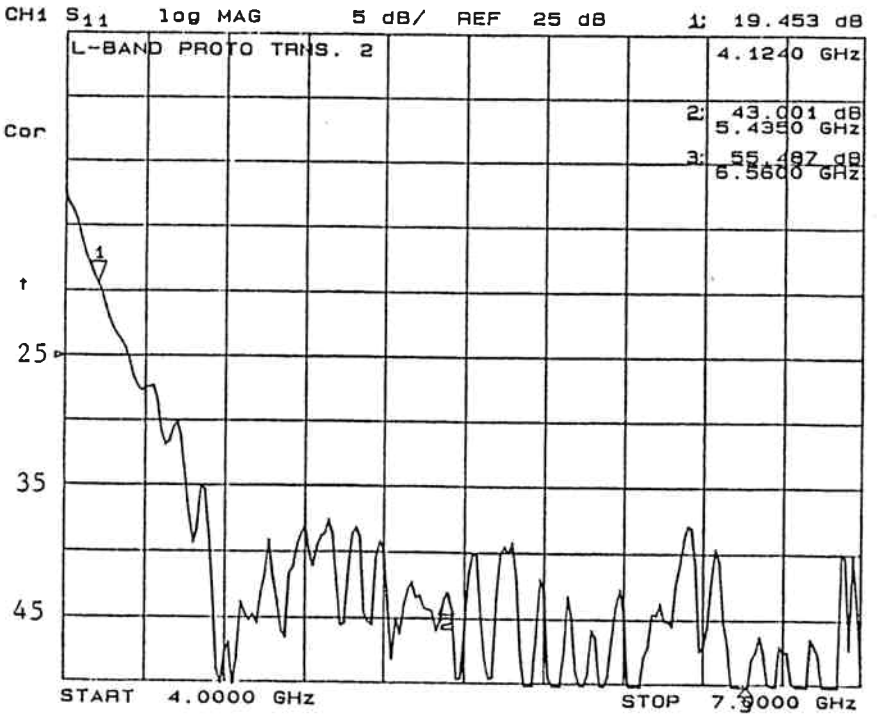

(b)

Fig. 6. Measured return loss of feed with
(a) taper #1 (Length = 33.140" at L-band) and
(b) taper #2 (Length = 20.550" at L-band).

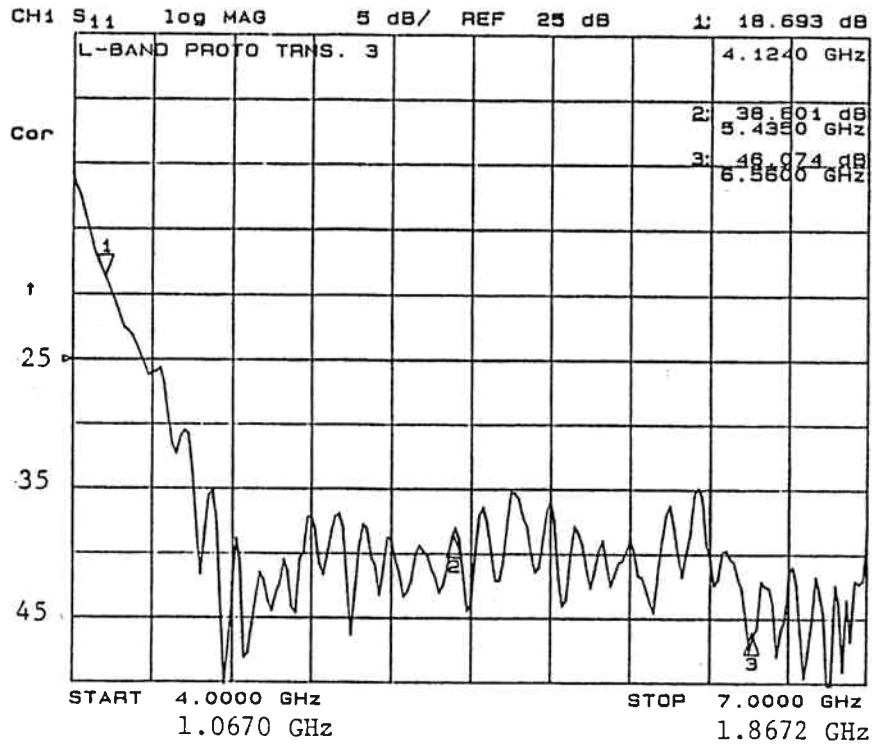

(a)

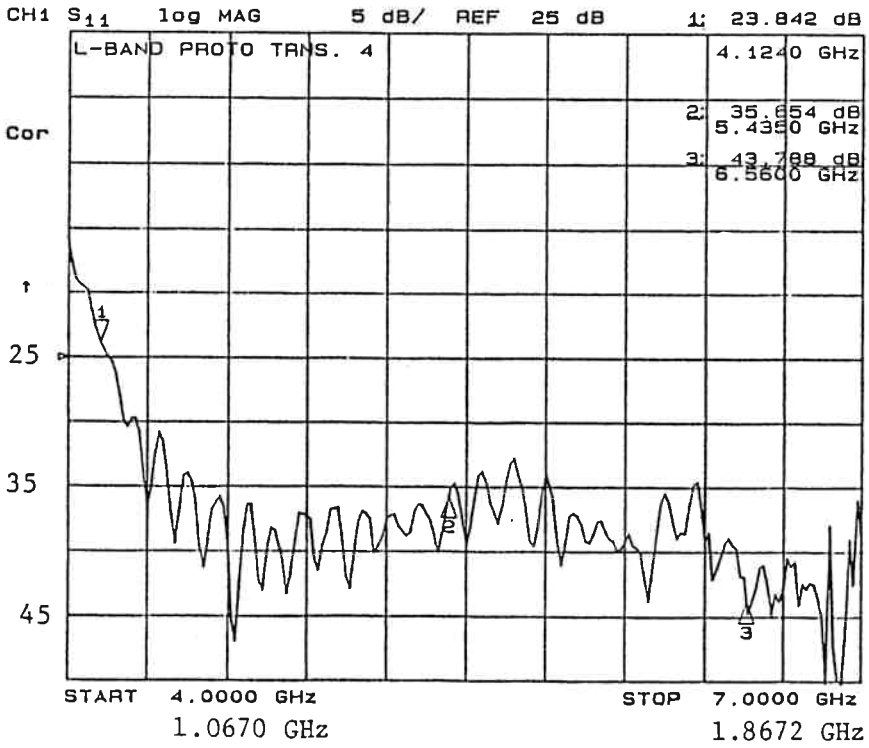

(b)

Fig. 7. Measured return loss of feed with
(a) taper #3 (Length = 20.550" at L-band) and
(b) taper #4 (Length = 20.550" at L-band).

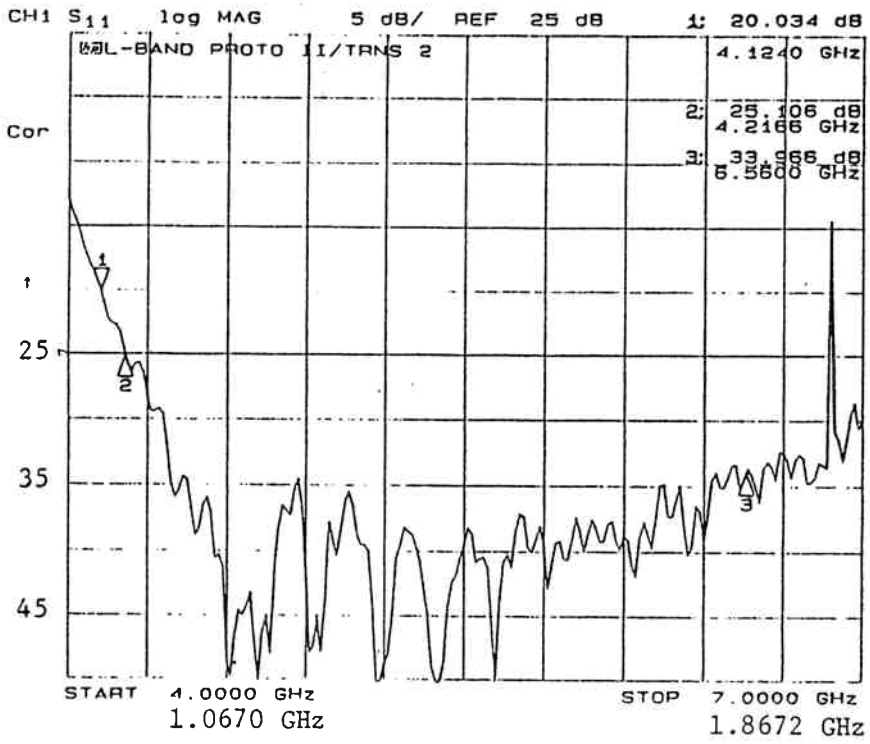

Fig. 8. Measured return loss of thin vane prototype with taper #2.